1. INTRODUCTION

1.1 STRUCTURE OF THE TECHNICAL DESIGN REPORT

Muons are an unmistakable signature of most of the physics LHC is designed to explore. The ability to trigger on and reconstruct muons at the highest luminosities is central to the concept of CMS, the Compact Muon Solenoid. CMS is characterized by simplicity of design, with one magnet whose solenoidal field facilitates precision tracking in the central barrel region and triggering on muons through their bending in the transverse plane. A perspective view of CMS is provided in Fig. 1.1.1(color), while transverse and side views, Figs. 1.1.2 and 1.1.3 (color) show the muon chambers in relation to the rest of the detector. (The color figures will be found at the end of the Report.)

The barrel muon chambers are drift tubes which provide a precise measurement in the bending plane, out to η=1.3. Since most of the return flux of the 4 T magnetic field is contained in the iron yoke, chambers with standard rectangular drift cells perform adequately.

At LHC energies, most events of interest will have one or more muons at higher rapidity, so the muon endcaps are of equal importance. Endcap chambers employ cathode strip chamber technology to provide high precision in the presence of a large and varying magnetic field, while their faster response time and finer segmentation allow them to function in the higher rate environment. A sophisticated alignment system relates the positions of the muon detectors to those of the central tracker elements to provide maximum momentum resolution.

The CMS muon system has a redundant and complementary trigger capability over nearly the entire rapidity range. A dedicated trigger element, the resistive plate chamber, will guarantee a fast, highly segmented trigger with a sharp p_T threshold and make it possible to achieve a very good understanding of trigger systematics.

The first two chapters constitute an “executive summary" of the Muon Technical Design Report and provide a synopsis of the remaining chapters. Chapters 3 through 7 describe in detail the principal hardware elements of the muon system In the first chapter of the TDR we summarize the physics goals of CMS and state the design requirements and special considerations, particularly background rates, which lead to specific choices for the detector parameters of the muon system. Short descriptions of the main detector elements follow.

Chapter 2, System Performance, presents in some detail the results of background studies, with particular emphasis on the impact of the various background sources on the muon detector elements. Studies of the momentum resolution of the full muon system over the entire rapidity range are given, and the salient aspects of the trigger performance are shown. We then put all the elements together in the simulation to show the muon system performance for representative physics processes, to demonstrate that the detector as designed can achieve the physics goals if the signals are there to be found.

Chapters 3 and 4 respectively describe the designs of the barrel Drift Tubes and the endcap Cathode Strip Chambers, giving particular emphasis to the R & D efforts that have led to these designs and describing test beam results that bear out the merits of the choices. System services and installation are also discussed in these chapters, as well as production plans, with emphasis on the tooling that has been developed for production runs.

Chapter 5, Resistive Plate Chambers, presents the status of the dedicated trigger elements, showing the substantial progress that has been made in adapting this technology to

the demands of the hadron collider environment. Preliminary results from the summer beam tests indicate that the baseline RPC design will function with an adequate safety margin in all the rapidity ranges of the detector.

Chapters 3 through 5 also describe the way in which each of these hardware elements generates trigger primitives, i.e., the lowest level pieces of information from each detector station containing position and/or angle information, that must be assembled into a coherent trigger. Chapter 6, Trigger and Data Acquisition, continues this process, showing how the primitives from each station are combined to indicate the presence of a potential track with the requisite qualities, p_T, isolation, etc., so that it can be considered a track candidate. Combining of information from the drift tubes, cathode strip chambers, and resistive plate chambers to form a global muon trigger is also described. Finally, a brief explanation is given of the process of identifying pieces of pipelined information from each detector element and reassembling them into a coherent event when the global trigger, either from the muon system or from another part of the CMS detector, requests that the event be read out.

Chapter 7, Alignment, presents a technological solution to the problem of aligning the barrel and endcap detectors among themselves, and the more complex problem of aligning these elements with respect to the inner tracker, so that the high momentum resolution capabilities of CMS can be realized. The alignment system must be able to cope with the deformation of the iron structure produced by the enormous magnetic forces. The physics solution to the alignment problem, alignment with muon tracks, is discussed as well.

Chapter 8, Control and Monitoring, gives a brief description of the organization of a system to monitor and control all relevant parameters of the muon system. This chapter is purposely generic since the objective is to achieve commonality, not only across detector subsystems, but indeed across the different experiments, to reduce costs and complications of this necessary but straightforward function. We attempt to show here that we have made a complete itemization of the quantities that must be monitored and controlled for each subsystem. Chapter 9, Safety, proceeds with the same philosophy, applying a common viewpoint to the various subsystems, again seeking an exhaustive enumeration of the areas of concern.

Chapter 10, Radiation Environment, presents three different approaches to the modeling of backgrounds, at different levels of sophistication, and the results are compared to give some idea of the level of uncertainty involved in background discussions. More detailed results regarding the background studies are also presented in this chapter. Chapter 11, Project Organization, lists the groups involved in the muon project and their areas of responsibility. Costs and schedules are presented in tabular form.

1.2 PHYSICS GOALS

As the Large Hadron Collider (LHC) pushes both energy and luminosity frontiers to open up discovery potentials, quality muon detection becomes a vital experimental design consideration. From its earliest conceptual stages, robust and precise muon detection has been the central theme (and the middle name) of the Compact Muon Solenoid experiment.

In the tremendously successful Standard Model of elementary particles, the interactions of the fundamental fermions – leptons and quarks – are mediated by gauge bosons obeying SU(3) x SU(2) x U(1) symmetry. More specifically, the electroweak interaction is described by spontaneously broken SU(2) x U(1) gauge symmetry. This leads to the emergence of massive vector bosons, the W and Z, which mediate the weak interaction, while the photon of the

electromagnetic force remains massless. It also leads to the existence of a scalar Higgs field with a non-zero expectation value. The Higgs Boson is virtually the only missing link in the theory, and the currently expected value for its mass is less than about half a TeV. At the LHC center-of-mass energy of 14 TeV, experiments will probe the entire allowed mass range for the SM Higgs boson and either discover it or be able to exclude it.

As experiments probe deeper into matter, exploring ever smaller distances, the corresponding cross-sections become smaller. Given the LHC energy of $\sqrt{s}$=14 TeV, collider luminosity becomes a very important factor in the discovery potential. Unfortunately, high luminosity also means high rates of background. At the LHC luminosity of $10^{34}cm^{-2}s^{-1}$, there are an average of about fifteen hadronic interactions per bunch crossing

Muon detection is the most natural and powerful tool to detect interesting events over the background. A “gold plated" signal of the Higgs Boson is its decay into Z-Z or Z-Z* which in turn decays into four charged leptons. If the leptons are muons, the best 4-particle mass resolution can be achieved, and muons are less affected than electrons by radiative losses in the tracker material. For example, in a 150 GeV Higgs event, Fig. 1.2.1, the muons stand out after the high magnetic field and absorbers filter out the large background of hadrons or non-isolated muons. Such an example underscores the discovery power of muon final states as well as the need for wide angular coverage for muon detection. The four-lepton channel is crucial for the discovery of the SM Higgs boson in the mass range from ~130 GeV up to ~750 GeV.

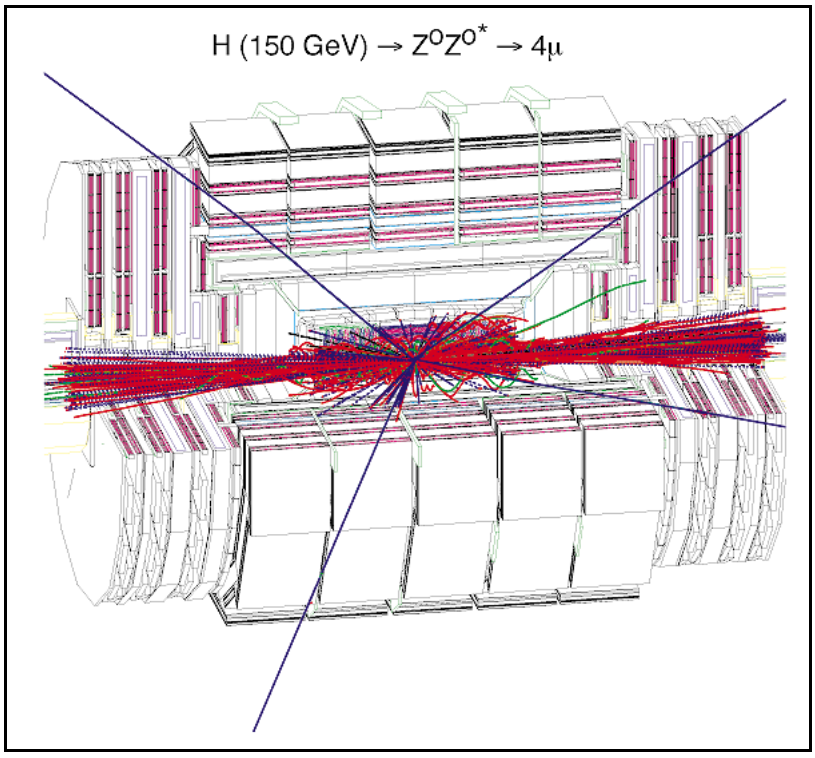

Fig. 1.2.1: A 150 GeV Higgs event decaying into four muons in the CMS detector.

Possible extensions of the Standard Model lead to the existence of other gauge fields. The LHC allows the discovery or exclusion of new gauge bosons with masses below ~4 TeV – more than an order of magnitude heavier than the W and Z. For the highest discovery reach, precision measurements of high energy muons (p_T > 1 TeV) in $Z' \to \mu^+\mu^-$ are important. Furthermore, sign determination for high energy muons is an essential tool to discriminate among various heavy gauge boson models giving different forward-backward asymmetries.

Lepton and photon isolation criteria are essential to extract most of the signals searched for at the LHC. Since muons can be measured within jets, which is generally not the case for electrons and photons, muons make it possible to determine directly the lepton and photon isolation rejection factors. The possibility of measuring muons in jets is also a powerful tool for b-jet tagging, exploiting the $b \to \mu$ decay, which is essential in a number of Higgs studies, top studies, and SUSY searches.

An appealing extension of the Standard Model is Supersymmetry: it allows the unification of the three couplings of the gauge interactions at a very high energy scale. Superpartners for all the presently observed particles are expected at the TeV mass scale. There are also multiple Higgs bosons. In the Minimal Supersymmetric Model for example, these are designated h^0, H^0, A^0, and $H^\pm$. At the LHC, Supersymmetry will be probed over the entire theoretically plausible mass range. Muons are again an essential tool not only for the discovery of these supersymmetric particles, squarks, gluinos, sleptons, etc., but also in determining their properties. An example is the cascade decay of neutralinos to di-muon pairs which yields an extremely well-determined mass difference between the two lowest lying neutralinos, which in turn allows the determination of the lowest supersymmetric particle mass and the reconstruction of $\tilde{q}/\tilde{g}$ masses.

The four-lepton channel is essential in the search for the MSSM Higgs bosons in the reactions $H \to ZZ^*$, $ZZ \to 4l^\pm$ ($4\mu^\pm$) at low tanβ (~2). The search for h, H, $A \to \mu^+\mu^-$ is the best way to explore the high tanβ (~30) region of MSSM parameter space. All these are narrow states (Γ<2 GeV) with expected masses in the ~100-500 GeV range, and detector acceptance and the excellent $2\mu^\pm$ and $4\mu^\pm$ mass resolution is of crucial importance. Large portions of the MSSM parameter space (tanβ, M_A) can also be explored with τ leptons using h, H, $A \to \tau\tau$ or $H^\pm \to \tau^\pm\nu$ modes. The $\tau \to \mu$ decays provide the most appropriate trigger for these channels.

The LHC is a copious source of t-quarks, with ~10^7 $t\bar{t}$ produced per year ($10^5 pb^{-1}$). Top events will largely be triggered through muon triggers ($t \to W \to \mu$) and effectively selected with b-jets tagged again with muons in jets, which is practically impossible with electrons. B hadrons are produced very abundantly as well. In the initial operation period of about 2 years, the integrated luminosity may not exceed ~$10^4 pb^{-1}$, and B-physics may be our main subject of study. Using $B^0_d \to \Psi\, K^0_S \to \mu^+\mu^-\, K^0_S$ or $B^0_d \to \Psi\varphi \to \mu^+\mu^-\, K^+\, K^-$ with μ tag events, significant measurements of CP violation will be possible. Investigation of $B^0_S \to \mu^+\mu^-$ with sensitivities up to BR≈10^{-9} will probe significantly FCNC scenarios. Most of the possible B^0_S oscillation measurements, for example using $B^0_S \to \Psi\, K^* \to \mu^+\mu^-\, K\pi$ with μ tag, rely either on $\Psi \to \mu^+\mu^-$ or more generally on some muon tagging technique.

The capability of the CMS detector to detect and trigger on low momentum muons will allow reconstruction of $\Upsilon, \Upsilon', \Upsilon'' \to \mu^+\mu^-$ in heavy iron collisions and make it possible to compare their relative production rates for various nuclei and in pp collisions. These relative suppression measurements are among the most promising tools to investigate quark-gluon

plasma formation. Detection of $Z \rightarrow \mu^+\mu^-$, even in the most crowded environment, opens up new possibilities in the field of heavy ion collisions.

1.3 PERFORMANCE REQUIREMENTS

The muon system has three purposes: muon identification, muon trigger, and muon (signed) momentum measurement. Performance requirements follow the physics goals, including the maximum reach for unexpected discoveries, and the background environment of LHC at its highest luminosity. A robust 4 T solenoid-based system is the key to the CMS design. Comprehensive simulation studies have indicated that the physics goals can be achieved if the muon detector has the following functionality and performance:

- MUON IDENTIFICATION: at least 16 λ of material is present up to η=2.4 with no acceptance losses.
- MUON TRIGGER: the combination of precise muon chambers and fast dedicated trigger detectors provide unambiguous beam crossing identification and trigger on single and multimuon events with well defined p_T thresholds from a few GeV to 100 GeV up to η=2.1.
- STANDALONE MOMENTUM RESOLUTION from 8 to 15% $\delta p_T/p_T$ at 10 GeV and 20 to 40% at 1 TeV.
- GLOBAL MOMENTUM RESOLUTION after matching with the Central Tracker: from 1.0 to 1.5% at 10 GeV, and from 6 to 17% at 1 TeV. Momentum-dependent spatial position matching at 1 TeV less than 1 mm in the bending plane and less than 10 mm in the non-bending plane.
- CHARGE ASSIGNMENT correct to 99% confidence up to the kinematic limit of 7 TeV.
- CAPABILITY OF WITHSTANDING the high radiation and interaction background expected at the LHC.

1.4 DESIGN CONSIDERATIONS

1.4.1. Backgrounds

As Fig. 1.4.1 shows, the major backgrounds occur at large η. Thus the chambers most affected by backgrounds are in the endcaps. Analysis of background sources has shown that the most critical regions in the background-generating process are the CMS beam pipe and the forward region, i.e., HF and the collimator with their shielding. The first three layers of CSCs see mostly beam-pipe generated background and punchthrough from the calorimeters. The last layer of chambers, ME4, catches particles created inside the forward calorimeter, HE (for ME4/1) and the collimator region (for ME4/2).

Background fluences on the chambers can be classified as follows:

- Low energy radiative electrons following slow neutron capture near or inside the muon chambers. These neutrons originate from hadronic cascades starting somewhere in the detector or in accelerator components.
- Charged hadrons from hadronic cascades: backsplash from HF and albedo, and leakage from HE and the collimator shielding.
- Decay muons coming mostly from the π/K decay inside the central cavity.
- Muons and other particles created in the accelerator tunnel after beam losses.

Various shielding configurations have been simulated for their effect on the baseline chamber design. Background rates of charged hadrons, muons and electrons on the muon chambers are shown in Figure 1.4.1. This figure was calculated using the current baseline design for the shielding at small angles. Further optimization of the local shielding around each muon station and at η~2.4 is in progress and is described in Chapter 10. It may decrease the local background rate of the soft electron component produced by neutrons by a factor of two. The total background rate at the highest pseudorapidity reaches up to 1 kHz/cm^2 at ME1/1 and ME4/1 and 0.4 kHz/cm^2 at ME2/1 and ME3/1.

Rates on other endcap and all barrel chambers are much less, in the range of a few tens of Hz/cm^2. High energy background (charged hadrons and muons) coincides in time with the bunch crossing; low energy background (electrons) is uncorrelated. These results are discussed in greater detail in the following chapter, while specifics of the simulations are the subject of Chapter 10.

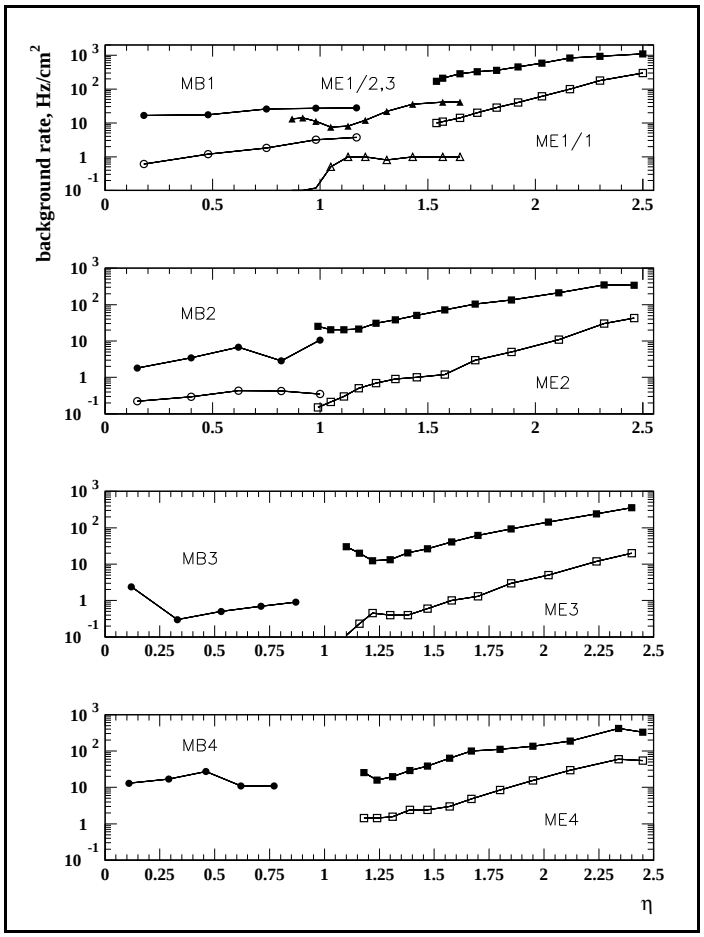

Fig. 1.4.1: Background fluences as a function of pseudorapidity, for each muon station. Solid points are the total fluence, open points are for the charged particle background.

1.4.2 Rates and trigger

With the design LHC luminosity of 10^{34}cm^{-2}s^{-1}, a bunch crossing frequency of 40 MHz and inelastic pp cross section at $\sqrt{s}$=14 TeV of 55 mb, one can expect on average ~15 pp

collisions per bunch crossing. The initial rate of 40 MHz has to be reduced by the First Level Trigger down to 30 kHz by looking for objects like muons, electrons/photons, jets, missing transverse energy and total transverse energy. One can roughly assume an equal sharing of this bandwidth between muon and calorimeter triggers.

Higher level triggers formed by a farm of commercial processors called the Event Filter have to reduce the rate further down to about 100 Hz, in order to match the bandwidth of a mass storage device (e.g. tape). The Event Filter input is designed to be able to accept 100 kHz of events to ensure a safety margin with respect to the expected 30 kHz delivered by the First Level Trigger.

On average, one per several hundred events will contain a muon which can enter the muon system (p_t>2-4 GeV, $|\eta|$<2.4). The resulting rate of 10^7 Hz is far too high for the Second Level Trigger. Therefore the First Level needs not only to recognize a muon but also to apply a momentum cut on single muon candidates. The p_T cut of 20 GeV is enough to reduce the rate to about 1 kHz. However, having in mind the presence of background and uncertainty on the cross sections, one should provide the possibility of raising this threshold to 50-100 GeV in order to maintain the rate at an acceptable value. On the other hand, for the two-muon trigger and in low luminosity runs, one can allow much lower p_T thresholds, down to the ranging-out limit of p_T ~4 GeV. Physics considerations discussed above and some technical limitations lead to the following list of guidelines for the muon trigger design:

1.4.2.1 Flexibility

In order to access all the interesting physics channels and to tune the rate to the level acceptable for the Event Filter, the p_T threshold must be adjustable. In the present design the full range from 2-4 to 100 GeV is covered.

1.4.2.2 Time resolution

The First Level Trigger must be able to assign an event to the proper bunch crossing. Thus the time resolution should be smaller than the bunch crossing interval, i.e. 25 s.

1.4.2.3 Speed

The trigger decision must be available about 3 μs after the collision. This includes propagation time of the signals from the detector to the Control Room (~120 m) and back.

1.4.2.4 High acceptance

Searches for rare events require an acceptance close to 100%. Therefore the muon stations are arranged in such a way that most tracks cross 4 triggering planes but every track crosses at least 3 triggering planes.

1.4.2.5 Redundancy

The trigger system has to deal properly with all possible inefficiencies, noise, accidental pileup and background from muon radiation. Thus it has to have substantial redundancy. In CMS this is ensured by having two complementary subsystems, one based on fast dedicated trigger detectors, namely Resistive Plate Chambers, and the other using precise multilayer muon chambers: Drift Tubes and Cathode Strip Chambers. This complementary is discussed in Chapter 6. For the specific needs of low p_T (~3-5 GeV) muon physics, such as B physics and heavy ion collisions, a double system of RPCs is included in the two innermost muon stations at the barrel.

1.4.3 Detector elements

Before describing the detector elements, we list the principal factors which argue for the choice of technology that has been made for the barrel and endcap muon measuring systems and the dedicated trigger devices.

1.4.3.1 Barrel

The choice of a drift chamber as tracking detector in the barrel was dictated by the low expected rate and by the relatively low intensity of the local magnetic field. A tube as the basic unit was preferred in order to have natural protection against damage from a broken wire and to partially decouple contiguous cells in the presence of electromagnetic debris accompanying the muon itself. Just as the iron thickness decouples two consecutive stations, so the relatively thick walls of the drift tubes, 2 mm, gives an effective decoupling among the several layers of tubes inside the same station. The simplest solution was to assemble together all the tubes in each slot of the barrel iron yoke to form a single rigid structure called a drift tube chamber.

Since the first studies of the drift tube design, it was realized that a group of three consecutive layers of thin tubes, staggered by half a tube, had an excellent time-tagging capability. A time resolution of a few nanoseconds can be obtained using signal processing based on simple meantimer circuits, which in the case of LHC makes it possible to have efficient local standalone bunch crossing identification.

The cell design makes use of four electrodes to shape an effective drift field: two on the side walls of the tube, and two above and below the wires on the ground planes between the layers. With this arrangement the requirement of 250 micron resolution per layer (which guarantees 100 microns per chamber) can be obtained while operating the tubes at atmospheric pressure with a binary Ar/CO_2 gas mixture. The multielectrode design ensures this performance even in the presence of the unavoidable stray magnetic fields present in the chamber region.

1.4.3.2 Endcaps

The cathode strip chamber has been chosen for the endcaps since it is capable of providing precise space and time information in the presence of a high magnetic field and high particle rate. CSC modules containing six layers provide robust pattern recognition for rejection of non-muon backgrounds and efficient matching of external muon tracks to internal track segments.

A strip width wider than the conventional width for CSC was chosen to limit the number of channels. Tests showed that if such strips were properly staggered in the module, a spatial resolution consistent with the multiple scattering limit could be obtained. Similarly, the wire spacing is somewhat larger than what has been used heretofore, but again tests showed that timing resolution was still adequate for bunch crossing identification.

The configuration of a CSC also easily allows chambers to be built to fit into the disk structure of the endcaps. Since the precision of the chambers derives from the strip pattern milled on their surfaces, an external reference can easily be provided to facilitate surveying and alignment.

1.4.3.3 RPCs

Resistive plate chambers have a very fast time response, comparable in fact to scintillators. Consequently they can provide an unambiguous assignment of the bunch crossing. However since they do not demand a costly readout device such as a photomultiplier, they can

be sufficiently highly segmented to make it possible not only to measure transverse momentum, but to do it at trigger time. Thus RPCs constitute a fast dedicated trigger which can identify candidate muon tracks and assign the bunch crossing with high efficiency.

While drift tubes and CSCs protect themselves against backgrounds by requiring coherent track stubs in multilayered modules, RPCs count on their fast response and segmentation to do so. Thus they have a different sensitivity to background. The higher rate capability of the new generation of detectors operating in avalanche mode makes their use at LHC feasible.

1.5 DETECTOR DESCRIPTION

1.5.1 Detector layout

The muon system uses three different technologies to detect and measure the muons; drift tubes (DT) in the barrel region, cathode strip chambers (CSC) in the endcap region, and resistive plate chambers (RPC) in both the barrel and endcap. A muon trigger in the barrel region is generated using a mean-timer to identify patterns. In the endcap the trigger is generated from the cathode readout patterns and the wire timing. For both barrel and endcap the RPCs provide an additional trigger signal which has a different sensitivity to backgrounds. All the muon chambers are aligned roughly perpendicular to the muon trajectories and distributed to provide hermetic coverage over the η range from 0 to 2.4. The barrel DTs cover roughly from $\eta = 0$ to $\eta = 1.3$ while the endcap CSCs cover from $\eta = 0.9$ to $\eta = 2.4$. The RPCs cover the region from $\eta = 0$ to $\eta = 2.1$. Some of the salient facts about these chambers are summarized in Table 1.5.1.

1.5.2 Barrel region

The barrel muon system of the CMS detector consists of four stations integrated in the return yoke of the magnet. Two stations are mounted on the inner and outer face of the yoke; the remaining two are located in slots inside the iron. The segmentation of each station is dictated by the longitudinal segmentation of the iron in five rings, each 2.5 m long, and by the presence of the azimuthal ribs needed to support the coil cryostat and the barrel calorimeter, and to create the slots inside the iron. In total, 60 chambers compose each one of the inner three stations, while 70 chambers are used in the outer station due to the presence of the yoke feet.

The basic sensitive element of the chambers is a drift cell of approximately 400 ns maximum drift time. This choice reduces the total number of wires to less than 200,000, while still keeping the occupancy negligible.

The twelve planes of drift tubes present in every chamber are organized in three independent subunits called Super Layers (SL) made up of four planes with parallel wires. Two SLs measure the coordinate in the bending plane (ϕ SL), the third measures the track coordinate along the beam (z SL). The two ϕ SLs have a separation of about 23 cm, in order to obtain the best angular resolution. This is the maximum allowed by the space available. Between them are the z SL and a thick honeycomb plate used as a spacer.

Within a SL, the four layers are staggered by half a cell, making it possible to use the correlation of the drift times in the different planes to compute the coordinate and the angle of the crossing tracks without any external time tag. The mean timer is fast enough to be used in the first-level trigger.

The obvious redundancy of the system, four stations of twelve planes each, makes it possible to cope with inefficiencies due to the dead zones which are caused by the supporting iron ribs, by the longitudinal space allowed for services, and by the non-negligible probability for a high energy muon to produce electromagnetic showers when exiting the iron slab.

1.5.3 Endcap cathode strip chambers

Each endcap region of CMS has four muon stations (ME1, ME2, ME3, ME4) of Cathode Strip Chambers (CSCs). These chambers have trapezoidal shape and are arranged in a series of concentric rings centered on the beam line. The stations are separated by the iron disks of the flux return yoke, which are thick enough to isolate the electrons in showers. Both YE1 and YE2 are 600 mm thick while YE3 is 250 mm thick. The last station is followed by a 100 mm thick iron disk whose primary purpose is shielding the ME4 station from backsplash backgrounds induced by particles scattered at small angle and interacting with the forward calorimeter, quadrupoles, beam pipe etc.

The ME1 station has three rings of chambers (ME1/1, ME1/2, ME1/3), at increasing radius, while the other three stations are composed of two rings of chambers (MEn/1 and MEn/2). All but the ME1/3 chambers overlap in φ and therefore form rings with no dead area in azimuth. In each of rings 2–4 there are 36 chambers covering 10° in φ at the outer radius, and 18 chambers covering 20° at the inner radius. The radial cracks between the chamber rings are not projective, and thus coverage, defined as at least 3 chambers on a muon path, is close to 100% down to θ=10° or η=2.4. The ME234/2 chambers, at the outer radius, are the largest - about 3.4 m long and 1.5 m wide.

ME1/1 chambers have to operate in an axial magnetic field in excess of 3 tesla, while ME1/2 chambers are in a highly non-uniform magnetic field of up to 1 tesla. The other chambers are generally in much lower magnetic fields. Most muons initially bend through the magnetic field and reach their maximum sagitta slightly in front of the first station. After this the muons are moving through the return flux and the sign of the bending is reversed. Consequently the sagitta measurement in the succeeding stations will be smaller. Therefore, the sagitta measurement at the first station is crucial and leads to more stringent requirements on the resolution and alignment in this station than in the other stations.

Each CSC has six layers of wires sandwiched between cathode panels. Wires run at approximately constant spacing, while cathode panels are milled to make six planes of strips running radially, one plane of strips per gas gap. Therefore, each chamber provides six measurements of the φ-coordinate (strips) and six measurements of the r-coordinate (wires). Strip width varies from 3 to 16 mm for different chambers, or from about 2 to 5 mrad in φ-coordinates. In the endcap geometry, measurement of track coordinates in the r-φ coordinate system is best suited for evaluating muon momentum. The precise φ-coordinate comes from interpolating charges induced by an avalanche on the strips. These charges are digitized and stored by the DAQ. The precision requirement for the endcap chambers is 75 μm for ME1/1 and ME1/2 chambers, and 150 μm for the rest (numbers are per six-plane chamber). Wires are grouped in 16-50 mm wide bunches and provide coarser radial information.

For trigger purposes, the position of hits in φ can be defined with a precision on the order of a tenth of a strip. First, the position of hits on each plane is determined to within a half-strip uncertainty, and then we use a look-up table to extract the most probable track coordinate corresponding to an observed six-plane pattern of the half-strips. The radial coordinate is available with an accuracy corresponding to a wire group width. Wire signals also provide

high-efficiency bunch crossing identification, the formal requirement being 92% per station. By picking the most frequent bunch crossing identification (BXID) out of four track segments from the four muon stations linked to one track, one can obtain better than 99% efficiency for correct bunch-crossing identification.

Overall, the Endcap Muon System consists of 540 six-plane trapezoidal chambers, with about 2.5 million wires, 210,816 anode channels and 273,024 precision cathode channels. A typical chamber has about 1000 readout channels.

1.5.4 Resistive plate chambers (RPC)

CMS has added planes of resistive plate chambers (RPCs) in both the barrel and endcaps to provide an additional, complementary trigger.

RPCs are gaseous parallel-plate chambers that combine a reasonable level of spatial resolution with excellent time resolution, comparable to that of scintillators. In the muon system, these chambers will cover roughly the same area as the DTs and CSCs but will provide a faster timing signal and have a different sensitivity to background. Trigger signals coming from the drift tubes, cathode strip chambers, and the RPCs will proceed in parallel until reaching the level of the global trigger logic. This will provide redundancy for evaluating efficiencies, and result in a higher efficiency and greater rate capability.

A resistive plate chamber is constructed of two parallel plates of material made of phenolic resin, with good surface flatness and a high bulk resistivity. Typically the plate separation is on the order of a few millimeters. The resin material is coated with a conductive graphite paint to form electrodes, and readout is made by means of aluminum strips outside the resin plates, insulated from the electrodes by some plastic material. In normal construction, two such assemblies are placed back to back, with the readout strips in the center. The entire sandwich is gas tight.

In their original concept, for data taking in cosmic ray applications, RPCs were run in streamer mode, in which the resulting pulses were large enough that no amplification stage was required. These large pulses however prevented high rate operation, since the electrode cell involved in the discharge process remained inefficient for the recharge time, which was long enough to limit operation to 100 Hz/cm^2. To use these devices in a high-rate environment, experimenters have begun to run their chambers in avalanche mode, with lower gas amplification and smaller pulses. The consequent drastic reduction of the elementary discharge cell has led to high rate capability, although now a robust signal amplification stage is needed.

Used in this way, RPCs constitute a fast dedicated trigger which can identify candidate muon tracks and assign the bunch crossing with high efficiency. Since they are low-cost devices, they can be sufficiently highly segmented to make it possible to measure the transverse momentum at trigger time. All these functions are ideal for the CMS application, and the higher rate capability of the new generation of detectors makes them feasible at LHC.

A total of six layers of RPCs will be mounted with the barrel chambers, two layers with each of stations MB1 and MB2, and one each in the outer stations. In the endcap region, each of the four layers of CSCs will have a layer of RPCs in conjunction with it, with their shape and method of mounting determined by the η segmentation. The RPCs will extend to η=2.1,

Prototype chambers representing the three technologies described above, drift tubes, cathode strip chambers, and resistive plate chambers, have recently been tested in a high radiation flux environment at the GIF facility at CERN. All three tubes of chamber have

performed according to design specifications in fluxes exceeding those expected at LHC. A photograph of the chambers in the test area is presented in Fig. 1.5.1 (color).

Table 1.5.1
Chamber properties and statistics

Detector	Drift Tubes	Cathode Strip Chambers	Resistive Plate	
Function	Tracking p_T trigger BXID	Tracking p_T trigger BXID	BXID p_T trigger Resolve tracking ambiguities	
η region	0.0 - 1.3	0.9 - 2.4	0.0 - 2.1	
Stations	4	4	Barrel 6	Endcap 4
Layers	RΦ 8, Z 4	6	2	
Chambers	250	540	360	252
Channels	195000	Strips 273024 Wire groups 210816	80640	80642
Spatial resolution (σ)	per wire 250 μm RΦ (6/8 pts) 100 μm Z (3/4 pts) 150 μm	RΦ (6 pts) 75 μm (outer CSCs) 150 μm R(6pts) (15-50)/$\sqrt{72}$ μm	Cell size	
Time resolution	5 ns	6 ns	3 ns	
Within 20 ns window	> 98% (station) no parallel B field	> 92% (station)	98%	

1.5.5 Trigger

The CMS Muon Trigger is based on three kind of detectors: Drift Tubes in the barrel, Cathode Strip Chambers in the endcaps, and Resistive Plate Chambers placed both in the barrel and the endcaps. They are arranged in the four muon stations in such a way that every muon with enough energy to penetrate through the detector material should cross at least three of them. The muon stations are interleaved with iron which serves as a return yoke for the CMS solenoid. Most of the iron is saturated at ~1.8 T, whereas the field inside the coil is 4 T. Bending in the field is used to measure the muon transverse momentum p_T.

RPCs are dedicated trigger detectors. Thanks to their excellent time resolution (σ~3 ns) they ensure precise timing. They are segmented in strips of $\Delta\eta\times\Delta\phi$ = ~0.1 × 5/16° = 20-100 cm × 1-4 cm, which makes possible a p_T measurement up to ~50 GeV. The measurement is done by the *Pattern Comparator Trigger* (PACT) which compares each pattern of hit strips to predefined patterns corresponding to various p_T values.

In the barrel there are 12 Drift Tube layers in each muon station. They are arranged in three quartets, two of them measuring ϕ and one measuring the Z coordinate. DTs can measure muon position (and thus p_T) more precisely than RPCs - 1.25 mm at the trigger level. The drift time is long (~400 ns) but the bunch crossing can be identified using a generalized meantimer technique. The *Bunch and Track Identifier* (BTI) circuit collects the drift time information from four layers of DTs and calculates the track position, angle and time by solving a system of linear equations. Results from two ϕ-layers are combined by a *Correlator*. Together with the Z-layer information they are sent through the *DT Trigger Server* to the *Track Finder*.

Each endcap muon station is equipped with a 6-layer CSC. Each layer contains radial cathode strips and wires perpendicular to them. At the trigger level the muon position is measured in each layer with half-strip precision (2-8 mm). A *Local Charged Track* is formed when a coincidence of ≥4 hit strips in different layers occurs. The strips must belong to a predefined road. A coincidence of ≥4 layers is also required for wires. It was found that the bunch crossing is best defined by the second hit in time. This is accounted for by the large spread of drift times with a maximum of 40–50 ns, by fluctuations in hit times and by accidental overlap with random background hits. As in the case of the drift tubes, a vector from each station is delivered to the *Track Finder*.

The Track Finder (TF) combines vectors received from the DT and CSC stations and forms full tracks with a defined p_T. Then the TF and PACT information is transferred to the Global Level-1 Trigger. Comparing TF and PACT data, the Global Trigger rejects some ghosts and background. Finally, once a track is identified, it applies p_T cuts to the muon candidates.

1.5.6 Alignment

The muon detector spectrometers are instrumented with optical alignment systems to constantly monitor the position and deformations of the muon chambers during detector operation. The aim is to provide position information of the detector elements with an accuracy comparable to the intrinsic chamber resolution, to be used as an off-line correction for track reconstruction.

The muon alignment scheme consist of two local stand-alone subsystems for the internal monitoring of the barrel and endcap muon detectors. To benefit from the highest momentum resolution capabilities of CMS, these subsystems are linked to the inner tracker alignment such that the position in space of the tracker detector and muon stations can be related at any time. The main design parameters are given in Table 1.5.2.

Following the specific detector configurations two different technical approaches have been chosen for the position monitoring of the barrel and endcap detectors.

The scheme for the barrel alignment system is based on the monitoring of the muon chambers position with respect to a network of radial reference structures, mechanically and thermally stable, fixed to the barrel yoke. They are optically connected between themselves, forming a closed reference network. The structures are equipped with video cameras which observe light sources mounted on the muon chamber fiducials.

Table 1.5.2
Alignment design parameters and component statistics.

Intrinsic sensor accuracy	<5 μm
Accuracy of barrel chamber positioning	<150-350 μm
Accuracy of endcap chamber positioning	<75-200 μm
Number of Rasnik systems	12
Number of MPA sensors	546
Number of video-camera detectors	612
Number of proximity measurements	1404

The alignment system of the endcap detectors uses straight-line monitors –Rasnik systems –to monitor the relative position of the four muon stations. The deformations of the CSC chambers are measured as well by optical straightness monitors defined across each layer of chambers.

Opto-mechanical angular and distance measurements and similar straightness monitors as for the endcap alignment are used to relate the inner tracker and muon detector alignment systems.

1.5.7 Magnetic field

The CMS Collaboration has chosen a solenoidal superconducting coil to generate a 4 T magnetic field over the entire tracking region. The inner diameter of the coil is 6.22 m, the coil is 13.48 m long. The tracking and calorimetry subsystems are completely enclosed within the field. The flux of the solenoid is returned by a set of iron disks in the endcaps and concentric twelve-sided cylinders in the barrel. The muon subsystem has four measurement stations in both barrel and endcaps, interleaved in the flux return region with the iron plates. This geometry serves to isolate background showers within one station as well as to provide an effective flux return. Details of the magnet construction are provided in the Magnet Technical Design Report [1.1].

Fig. 1.5.1 (color) shows the CMS magnetic field as calculated with the ANSYS® finite element program using an axisymmetric model. This figure shows a quadrant of the CMS detector with a constant 4 tesla field inside the solenoidal coil. An important advantage of ANSYS is its ability to use the magnetic field as calculated to compute the forces on the iron plates and the resultant deflection. Details of the magnetic modeling and the specific inputs to the calculation are given in a CMS Technical Note [1.2]. Fig. 1.5.2 (color) shows the radial component of the field, and we immediately see the effect of the gaps between the barrel rings as well as the large and rapidly changing radial field at the end of the coils. As a result, chambers in this area (ME1/2 and MB2/1) experience a large field variation.

Large forces on the endcap disks appear as a result of these magnetic fields. The overall magnetic force on the first endcap disk is roughly 7000 metric tons for an object that weighs about 900 metric tons, so the magnetic forces dwarf the gravitational forces even for such heavy disks. The result of the action of these forces is shown in Fig. 1.5.3 (color) where the center region of each endcap disk (including the nose) deflects toward the interaction region by roughly 14 mm.

The high field of the solenoid is the key to the very good momentum resolution of the detector, and at the same time the field confines some fraction of the low momentum particles to the beam pipe region so that they do not confuse the inner tracking. But from the point of view of the muon subsystem, the field sets the environment in which the detectors operate, and the large forces produced by the field mean that the iron structure in which the chambers are mounted cannot be regarded as fixed, so that alignment is an ongoing process.

The full field is present in the region in which the innermost endcap CSCs, the ME1/1 chambers, must operate. However, the field at this position is uniform and almost entirely axial, so that relatively simple measures can compensate for the effect of the field on the drift of the electrons. This is discussed in detail in Sections 4.3 and 4.8.

At the next endcap station going out radially, ME1/2, the field has fallen off to a considerable degree, but it is no longer uniform and no longer axial as shown in Fig. 1.5.4.

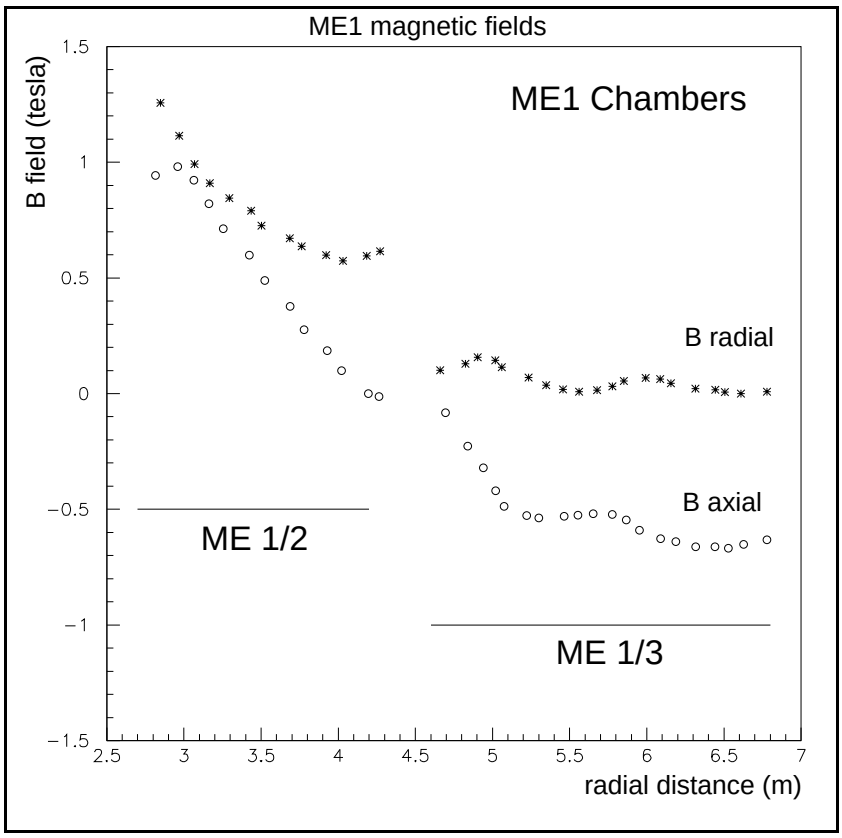

Fig. 1.5.4: Axial and radial components of the magnetic field in the vicinity of the endcap chambers ME1.

The radial component is the same as or greater than the axial component. Due to the large variation across the chamber, simple compensation schemes will not work. However, since the drift space in the CSC is small, the deterioration of resolution from the changing field components is also small, and the resolution of uncompensated chambers is within the requirements of the system.

Ideally the barrel drift tubes should be in a field-free region, since the return flux is largely contained within the iron. However, at the end of the coil and in the iron gaps there are large stray fields in the chamber area, as shown in Fig. 1.5.5. Near the end of MB2/1 the radial component reaches 0.8 tesla. This requires a rather complicated field shaping scheme in the DT cells, and in the worst regions results in a loss of resolution and bunch tagging efficiency. Fortunately, these regions are small with respect to the overall area covered by the DTs.

While most of the magnetic flux is returned via the iron plates, the fringe field outside the detector remains uncomfortably large. In Fig 1.5.6 we show the calculated field outside the solenoid in the z = 0 plane out to a radius of 50 m. In the region of R = 4-7 meters, the three cylindrical rings of iron plates are clearly visible, with a B field near saturation (~1.6 tesla). Outside the detector, at a radius of 8-9 m, where electronics will be located, the field is roughly 0.05 tesla (500 gauss). At larger distances of 35 m (roughly the location of the underground control room) the field is still 0.0005 tesla (5 gauss). Consequently we will require careful shielding of the electronics throughout the CMS underground hall.

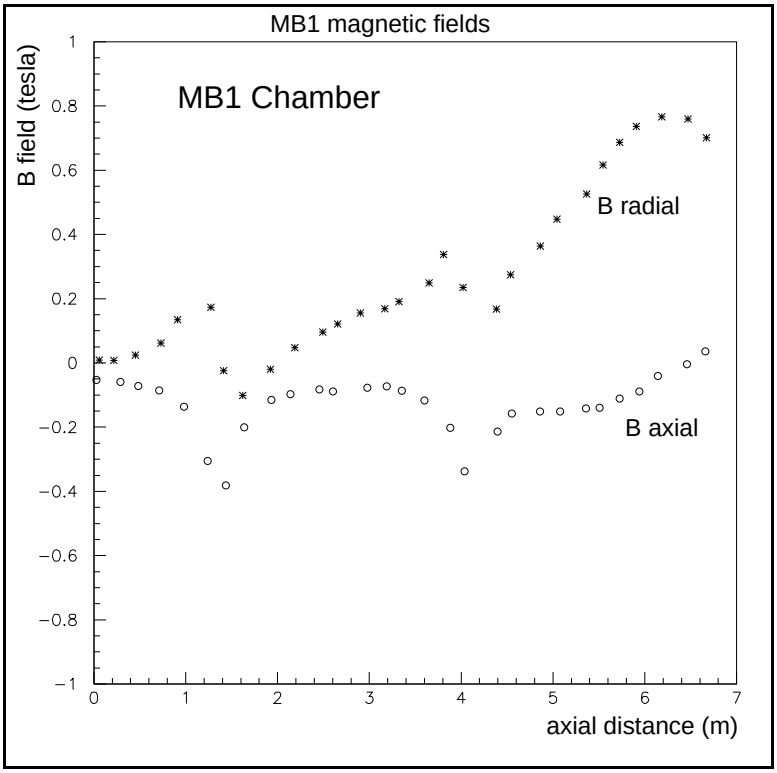

Fig. 1.5.5: Axial and radial components of the magnetic field in the vicinity of the barrel chamber MB1.

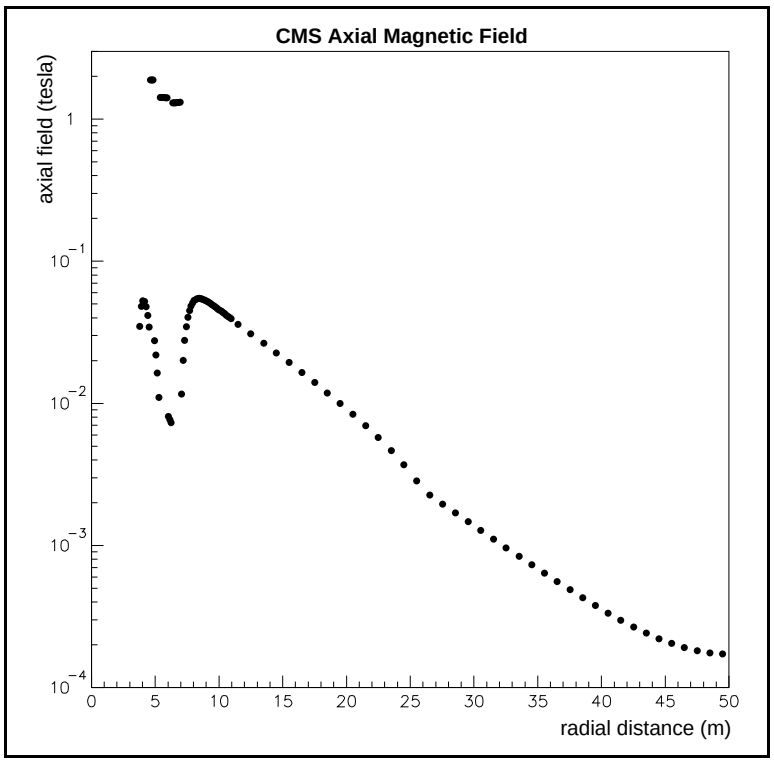

Fig. 1.5.6: Magnetic field moving out radially from the beam line in the z=0 plane. A non-negligible field exists at considerable distance from the detector.

1.6 PROJECT ORGANIZATION, SCHEDULE, AND COSTS

The CMS Muon Group comprises over 400 physicists and engineers from nearly 50 institutes in 13 countries. Its task is to design, construct, and utilize detectors for the identification and measurement of muons in the barrel and endcap regions, and to link those devices to the central tracking instrumentation to form a coherent whole.

1.6.1 Organization

The Muon Group follows the organizational scheme of CMS as a whole. It operates under a constitution which sets up an Institution Board as the highest level decision-making body for the group. This board, headed by a chairman and a deputy chairman, each elected for two-year terms, has as its charge to ratify decisions made by the Technical Board, and to see to it that the resources available to the group are best matched to the demands of the project.

The Technical Board is headed by Project Managers appointed by the CMS Spokesman. Because the barrel and endcap sectors of the detector are in very different regimes of background and operational environment, the Technical Board is divided into two functional units, one for the barrel and one for the endcap. As a consequence of the formation process of CMS, these two units correspond also to a geographical division, the barrel part being largely the responsibility of institutes from CERN member states, and the endcap part the responsibility of US and RDMS institutes. The two Project Managers are members of the CMS Management Board.

Each Project Manager is assisted in his task by a Technical Coordinator in directing the work of subgroups responsible for chamber construction, electronics development, trigger, alignment, integration, software and simulation, and testing. Subsystem Coordinators make up the balance of the Technical Board. The two technical coordinators are members of the CMS Technical Board. Because of the rather independent nature of the barrel and endcap projects, the Technical Boards of each subproject function separately for the most part; they provide a forum for technical discussions and formulate proposals and recommendations for the Muon Institution Board.

1.6.2 Responsibilities

Detailed breakdowns of the responsibilities of the institutions for each subproject are provided in Chapter 11. Because of their global character, questions of software and simulation, alignment, integration, and trigger are to a large degree common, and the subgroups in charge of these areas are formed by individuals from both parts of the overall group.

Detailed planning and scheduling is carried out by the CMS Management Board in consultation with the Muon Technical Board. However, in general terms, the construction phase begins in early 1999 and reaches completion in 2003. Since one endcap must be lowered into the experimental hall before the other, half of the endcap chambers, complete with electronics, must be ready for above-ground installation before 2003. Chapters 3 and 4 discuss in detail the progress of prototypes. Both the barrel and endcap groups are now beginning the construction of "pre-production prototypes" which will be for all practical purposes part of the production sequence.

1.6.3 Costing

Detailed cost estimates have been presented in successive Cost Books, and the current state of these estimates is summarized in Chapter 11. Consistent with the overall cost ceiling on CMS of 475 MCHF, the Muon Project is capped at 61.3 MCHF. Cost estimates developed to this point are consistent with this number, and the available resources are adequate, within the uncertainties, to complete the project. For the endcap sector, the manpower costs are either included in the scope of the project or are counted against the base programs of the institutes involved. For the barrel sector, manpower costs come under the scope of the Memoranda of Understanding. In either case, the Muon Group considers the financial and manpower resources to be sufficient to bring the project to completion.

1.7 ASSUMPTIONS REGARDING OTHER CMS DETECTOR ELEMENTS

Although many assumptions are made in this TDR regarding the performance or characteristics of other element of the CMS detector, e.g., the inner tracker resolution in the calculation of the combined tracking resolution (Fig. 2.3.2), we wish to explicitly mention the assumptions made in the discussion of a) the background levels around the CSCs, and b) the link system of the alignment.

All calculations of background levels and occupancies of the CSCs, in particular of ME4, assume that a 10 cm iron disk, of roughly the same shape as the flux return disks, is installed between ME4 and the forward hadron calorimeter HF and the low-beta quadrupole magnets. The exact location of this disk is shown in Fig. 2.1.1.

The current scheme for the link between tracker and muon detectors, as described in Section 7.3, assumes a tentative baseline design for the inner tracker. Nevertheless the final implementation will follow the design optimization of the tracker detector and will be described in the CMS Tracker Technical Design Report, to be published in early 1998.

References

[1.1] The Magnet Project Technical Design Report, CERN/LHCC 97-10, May 1997.

[1.2] R. Loveless and F. Feyzi, Magnetic and Structural Analysis of the CMS Endcaps, CMS TN/94-293, December 1994.